Available online at www.sciencedirect.com
SCIENCE DIRECT®
Thermochimica Acta 431 (2005) 205–211
thermochimica acta
www.elsevier.com/locate/tca

Phase transitions in dipalmitoylphosphatidylcholine–water and dipalmitoylphosphatidylcholine–$CaCl_2$ aqueous solution system by means of a high resolution and high-sensitive differential scanning calorimeter

Hideko Hayashi *, Ken-ichi Tozaki, Chiaki Ikeuchi, Hideaki Inaba

Faculty of Education, Department of Education, Chiba University, 1-33 Yayoi-Chou, Inage-ku, Chiba 263-8522, Japan

Received 21 October 2004; received in revised form 10 April 2005; accepted 14 April 2005
Available online 23 May 2005

Abstract

The phase transitions of dipalmitoylphosphatidylcholine (DPPC)–water and DPPC–$CaCl_2$ aqueous solution system were investigated in the both directions of heating and cooling process by means of a high resolution and high-sensitivity differential scanning calorimeter. The peaks due to the transitions showed different features between heating and cooling runs, especially for the pre-transition and the sample with a high Ca^{2+} concentration. A sub-main transition in multilamellar bilayers of DPPC was detected in addition to the pre-transition and the main transition. The addition of Ca^{2+} ion affected the pre-transition and the sub-main transition as well as the main transition.

Keywords: Heat flux; DSC; High resolution; Phase transition; Dipalmitoylphosphatidylcholine (DPPC); Sub-main transition; Ca ion

1. Introduction

In the dipalmitoylphosphatidylcholine (DPPC)–water system, their multilamellar vesicles (MLV) undergo a variety of thermotropic and lyotropic phase transitions [1–5]. The main-transition is the chain melting transition from a low temperature rippled-gel phase (P'_β) to a high temperature liquid crystalline phase (L_α) [1]. In addition to the main-transition, the multilamellar vesicles are known to undergo the pre-transition and sub-transition at lower temperatures. The pre-transition is a low enthalpy transition below the main transition from non-rippled gel-phase (L'_β) to the rippled-gel phase P'_β [6,7]. The sub-transition is a chain packing transition from the subgel phase (L_c) to the non-rippled gel-phase L'_β [8]. In addition to these phases, a metastable rippled gel-phase (P'_β(mst)) was reported to appear only in the cooling process from the liquid crystalline L_α phase according to the study using AC calorimeter and X-ray diffraction by Yao et al. [9–12]. The P'_β(mst) phase was not observed in the reheating process after cooling to the L'_β phase through the pre-transition. According to the study using AC calorimeter by Tenchov et al. [10], the excess heat capacity due to the main transition in the cooling process became considerably smaller than that in the heating process. They explained that the transition in the cooling direction was too slow to obtain the excess heat capacity as the equilibrium value by AC calorimetry. Therefore, it would be desirable to measure the phase transitions of the DPPC–water system calorimetrically in the cooling process as well as in the heating process at a reasonably slow scan rate with an enough sensitivity. In addition to these transitions, Jørgensen et al. [13–16] reported a sub-main transition for the diacylphosphatidylcholine having fatty acyl chains of 17–20 carbon atoms near the main transition. However, the sub-main transition for the diacylphosphatidylcholine having fatty acyl chains of 16 carbon atoms, which corresponds to DPPC, has not been reported yet.

* Corresponding author. Tel.: +81 432902604; fax: +81 432902604.
E-mail addresses: inabah@faculty.chiba-u.jp, hayashi@faculty.chiba-u.jp (H. Hayashi).

0040-6031/$ – see front matter © 2005 Elsevier B.V. All rights reserved.
doi:10.1016/j.tca.2005.04.020

The additive effect of salt on the phase transitions in DPPC–water system has also been reported by many investigators [13,14,17–24]. In these investigations, divalent cations, particularly Ca^{2+}, were reported to have an effect on both the enthalpy change and the temperature of the transitions. These effects are due to the interaction of cations with the lipids, which changes interbilayer force [25,26] and the arrangement of the multilamellar structure [19,20,27]. Therefore, to study the additive effect of salt on the phase transitions in DPPC–water system is also very interesting.

In this paper, we would like to present the detailed feature of the phase transitions of DPPC–water and DPPC–$CaCl_2$ aqueous solution system in the both directions of heating and cooling by means of a high resolution and high-sensitivity DSC.

2. Experimental

Synthetic 1,2-dipalmitoyl-sn-glycero-3-phosphocholine (DPPC) with the purity higher than 99% was purchased from Sigma Chemical Co. and used without further purification. Calcium chloride used was an analytical grade, which was purchased from Wako Pure Chemicals Japan. Water was purified using a Milli-Q-plus system (Millipore) and distilled in all-quartz apparatus before use.

Multilamellar lipid vesicles (MLV) were prepared by dispersing DPPC in water or aqueous solution of calcium chloride of 10 and 100 mM. DPPC concentrations were less than 55 wt.% in all preparation, which is the condition of excess water according to Kodama and Grabielle-Madelmont [4,5]. The sample of DPPC–water system was prepared by adding 5.93 mg of pure water to 2.66 mg of DPPC. The sample of DPPC-aqueous solution of calcium chloride was prepared by adding 2.88 mg of 10 mM $CaCl_2$ solution to 3.11 mg of DPPC and adding 9.00 mg of 100 mM $CaCl_2$ solution to 4.07 mg of DPPC. The molar ratio of Ca/DPPC for these samples was 0, 0.042 and 0.164, respectively. The dispersions were incubated at 325 K for 30 min and cooled to room temperature. This process for the dispersion was repeated several times using commercial DSC until measurements become reproducible.

The differential scanning calorimeter used was a high resolution and high sensitivity DSC, which is a simple version of the nW-stabilized DSC [28,29]. This apparatus lacks of an auxiliary heater to keep the central part of the calorimeter in a nearly adiabatic condition and the pairs of Cu blocks and thermoelectric modules to reduce the temperature fluctuation at the sample cell, which the nW-stabilized DSC has. Although this DSC has a less baseline stability than the nW-stabilized DSC, it has still at least one order of magnitude better baseline stability than the commercial ones. The baseline stability of the present DSC was ±150 nW. The schematic drawing of the DSC is shown in Fig. 1. The temperature difference between a sample and a reference material is measured by thermoelectric modules, TM1-1 and TM1-2, which are made of 17

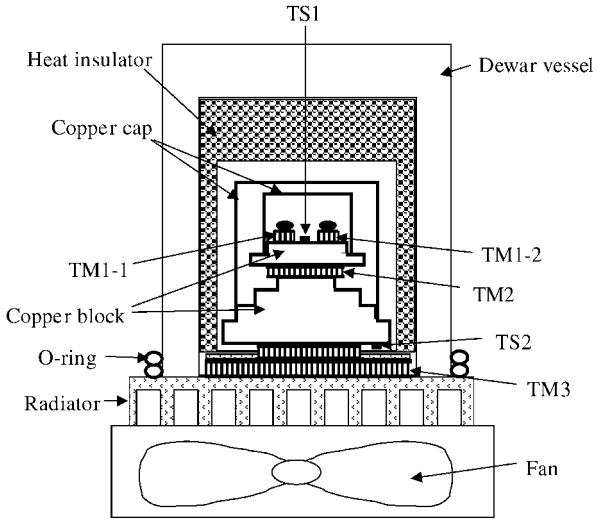

Fig. 1. Schematic drawing of the present DSC.

semiconducting thermoelectric elements connected in series and have an electromotive force of 7.4 mV K^{-1}. The temperature control was made using a Pt temperature sensor, TS2, by adjusting the current of the thermomodule, TM3. TM3 is made of semiconducting thermoelectric elements and can pump heat in either direction to heat or cool the copper block by changing the magnitude and the direction of the current through it, so that the measurements can be made in either direction of heating and cooling in this DSC. We calibrated the temperature of TS1 by measuring the resistance of TS1 as a function of the melting temperature of the standard materials, such as docosane (SRM 1973; NIST in USA), biphenyl (LGC 2610: LGC in UK) and water. Then, we know the temperature of the sample by measuring the resistance of TS1.

Since the thermal conductivity of the sample is usually low compared with that of metals, the sample container and the sample amount should be as small as possible in order to increase the resolution of the calorimeter. The sample container used was made of aluminum with 3.8 mm in diameter and 1.8 mm in depth. The total sample amount (DPPC + dispersing solution) used was about 10 mg and was quite smaller than that in the MicroCal, which has been commonly used to detect a small heat of the phase transitions of phosphatidylcholines [13–16,18,30,31]. The heating and cooling rate chosen was 2 mK s^{-1} (7.2 K h^{-1}).

3. Results and discussion

Fig. 2 shows the DSC curve of DPPC–water system at the heating rate of 2 mK s^{-1}. In Fig. 2, a baseline is shown in a dotted line, which was determined so as to connect the low temperature data smoothly to the high temperature ones. The first peak shows the pre-transition (non-rippled gel to the rippled gel) and the second large peak shows the main transition (rippled gel to liquid crystalline) of DPPC–water

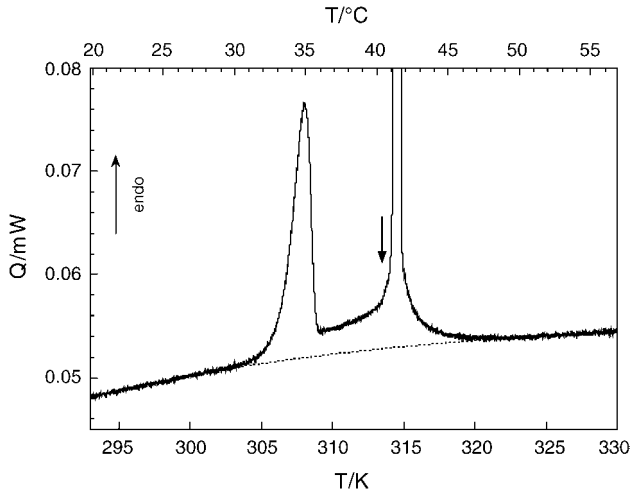

Fig. 2. DSC thermogram of DPPC–water system at the heating rate of 2 mK s^{-1} (7.2 K h^{-1}).

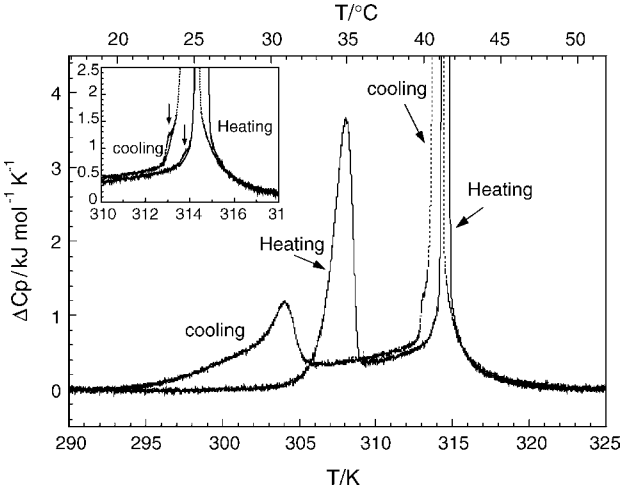

Fig. 4. The magnified figure of the excess heat capacity of DPPC–water system at the heating/cooling rate of 2 mK s^{-1} (7.2 K h^{-1}). The figure shown in the inset is the magnified one around 314 K. A small peak marked by an arrow shows the sub-main transition.

system. The excess heat flux of the peaks was obtained using the baseline shown in Fig. 2. Dividing the excess heat flux by the heating rate and the number of moles of DPPC, the excess heat capacity of DPPC–water system is obtained and shown in the bottom of Fig. 3(a), where that including Ca^{2+} is also shown upwards in a shifted vertical scale as a function of the Ca/DPPC ratio. The excess heat capacity as a function of the Ca/DPPC ratio obtained in the cooling direction is shown in Fig. 3(b).

The transition temperature of the main transition was slightly increased by the increase of the Ca^{2+} concentration, being in good agreement with that reported in the literatures [21–23,32,33]. This behavior is considered to be due to the interaction between Ca^{2+} and choline head group. The pre-transition is reported to merge the main transition at high Ca^{2+} concentrations[33].

Fig. 4 shows the magnified excess heat capacity near the pre-transition and the main transition of DPPC–water system both in the heating and cooling runs. Almost the same values were obtained between the heating and cooling runs at the temperatures near 293 and 320 K, indicating the excellent stability of the present DSC. The transitional peaks became broad in the cooling run as compared with the heating run. Especially for the pre-transition in the cooling run, the peak was very broad and seems to be composed of more than two peaks. Onset temperature of one peak is almost same for that in the heating run, which is about 305 K. Another peak is very broad and takes place between 307 and 295 K. It is considered that the metastable rippled gel-phase is not single state as considered in rippled gel-phase by Heimburg [6] and each

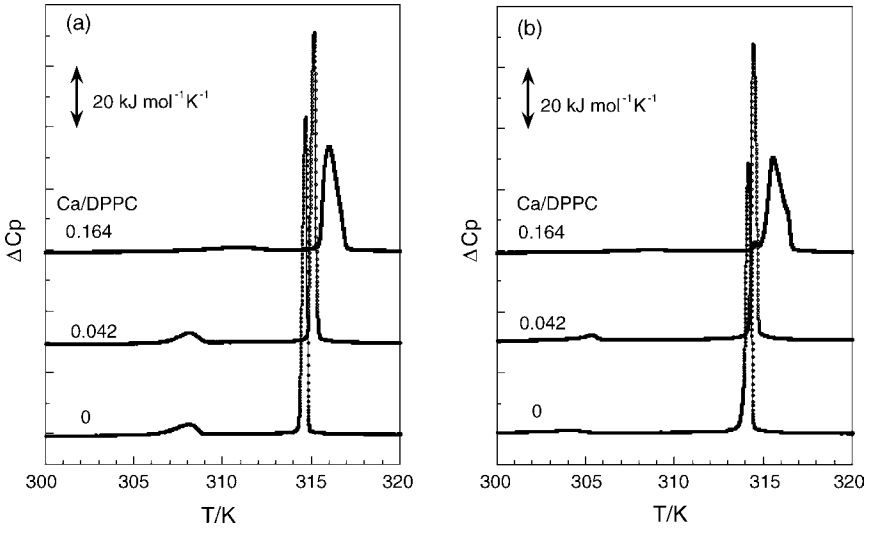

Fig. 3. Excess heat capacity of DPPC–water–$CaCl_2$ system at the heating/cooling rate of 2 mK s^{-1} (7.2 K h^{-1}): (a) heating run, (b) cooling run, the results with the different Ca/DPPC ratios of the sample are shown in the shifted vertical.

sate transits to the gel-phase individually with the different transition speed. Kato and Kubo [34] expected the existence of three states during the transition from the metastable rippled gel-phase to the gel-phase in the cooling process from the measurement of the temperature dependence of the transmitted light intensity. Yao et al. [9,11,12,35] reported that the transition from the metastable rippled gel-phase to the gel-phase in the cooling was considered to include a slow process. These reports are quite compatible with the present results although it is not apparent that broadening of low-temperature part of pre-transition peak is due to the slow process or multiple states which transited at different temperature in the peak.

The excess heat capacity of the rippled-gel phase P'_β was larger than that of the gel phase and the liquid crystalline phase both in the measurements of the heating and cooling process as seen in Fig. 4. The larger excess heat capacity of the rippled-gel phase was also reported by Blume et al. [35–38]. The larger excess heat capacity in the rippled-gel phase is considered to be due to the additional mode of molecular motion concerning the acyl chain conformation, such as the formation of fluid lipid line defects, as proposed by Heinberg [6]. It would be also possible to think that the larger excess heat capacity in the rippled-gel phase due to the additional mode of molecular motion is the onset of the main transition.

The transitional enthalpy change from the gel phase to the liquid crystalline phase is calculated using the baseline such as that shown in Fig. 2 and is listed in Table 1 as the total enthalpy change. The total enthalpy change obtained from the heating run was 40.6 kJ mol^{-1} and that from the cooling run was 41.1 kJ mol^{-1}, showing almost the same values. The total enthalpy change, 39.26 kJ mol^{-1}, obtained by Heimburg [39] is close to the present values. The enthalpy change of the main transition obtained from the cooling process, 36.3 kJ mol^{-1}, is slightly larger than that obtained from the heating process, 34.0 kJ mol^{-1}. Koynova et al. [35] obtained a similar value for the enthalpy change of the main transition obtained from the heating process, 33.3 kJ mol^{-1}. However, they estimated a smaller value in the cooling process, since they found a smaller value when the heating run of the DSC measurement started at 308 K after cooling from L_β phase, which is in the temperature region of the metastable rippled gel phase. The present value of the enthalpy change obtained from the cooling process is larger than their estimation. However, the reason is not known at present.

In the inset of Fig. 4, we can see a small peak as marked by an arrow in a low temperature part of the main transition both in the heating and cooling runs, which is considered to be due to the sub-main transition. Jørgensen et al. [13–16] observed the sub-main transition just below the main transition in the diacylphosphatidylcholines having fatty acyl chains of 17–20 carbon atoms by means of X-ray diffraction and the calorimetric measurement. From the fact that the enthalpy change of this transition became smaller as the number of carbon atoms 17–20 of the fatty acyl chains decreased, Jørgensen thought that the sub-main transition for the diacylphosphatidylcholine having fatty acyl chains of 16 carbon atoms (which corresponds to DPPC) was not detected [16]. No sub-main transition for DPPC–water system reported so far may be due to its very small peak. The detection of the sub-main transition in DPPC–water system shows the high resolution and high sensitivity of the present DSC. The sub-main transition was also detected in the cooling direction as seen in Fig. 4, which means that the sub-main transition has a reversible nature. Using the baseline shown in the inset in Fig. 4, the enthalpy change due to the sub-main transition was obtained to be 16 J mol^{-1}. This value is considerably smaller than that of diacylphosphatidylcholines with fatty acyl chains of 17 carbon atoms, 32 J mol^{-1} [16]. The enthalpy of the sub-main transition including DPPC-aqueous solution of calcium chloride is also listed in Table 1.

Fig. 5 shows the excess heat capacity of the DPPC–water–Ca sample with Ca/DPPC = 0.042. The excess heat capacity of the sample with Ca/DPPC = 0.042 shows only slight differences from that without Ca. The peak due to the sub-main transition of the sample with Ca/DPPC = 0.042 became none in the heating run, but it became larger in the cooling run. The low-temperature part of the pre-transition in the cooling run of the sample with Ca/DPPC = 0.042 became smaller than that without Ca.

Fig. 6 shows the excess heat capacity of the sample with Ca/DPPC = 0.164. The broadening of main peak in heating and cooling run is observed as seen in Fig. 3. In addition to this, the interval between the pre-transition and the main transition became smaller as the increase of the Ca content as seen from Figs. 4–6, as also reported by [17,23,40]. In Ca/DPPC, Inoko et al. [27] have carried out the structural studies using small angle X-ray diffraction. According to their results, the thickness of the water layer increases

Table 1
Phase transition temperatures and enthalpy changes of DPPC–water–$CaCl_2$ system

Ca/DPPC ratio		ΔH_{total} (kJ mol^{-1})	T_{pre} (K)	ΔH_{pre} (kJ mol^{-1})	$T_{sub\text{-}main}$ (K)	$\Delta H_{sub\text{-}main}$ (kJ mol^{-1})	T_{main} (K)	ΔH_{main} (kJ mol^{-1})
0	Heating	40.6	306.2	6.6	313.8	0.016	314.3	34.0
	Cooling	41.1	305.6	4.8	313.1	0.033	314.4	36.3
0.042	Heating	41.5	306.5	5.7	–	–	314.8	35.7
	Cooling	40.9	305.9	4.4	313.4	0.050	314.7	36.4
0.164	Heating	38.9	306.9	5.2	–	–	315.5	33.7
	Cooling	37.2	310.5	3.3	314.5	0.39	316.6	33.4

The sub-main transition temperature shown here is obtained from the peak temperature. The other transition temperatures are obtained from the intersection of the maximum slope of the peak and the baseline (onset temperature).

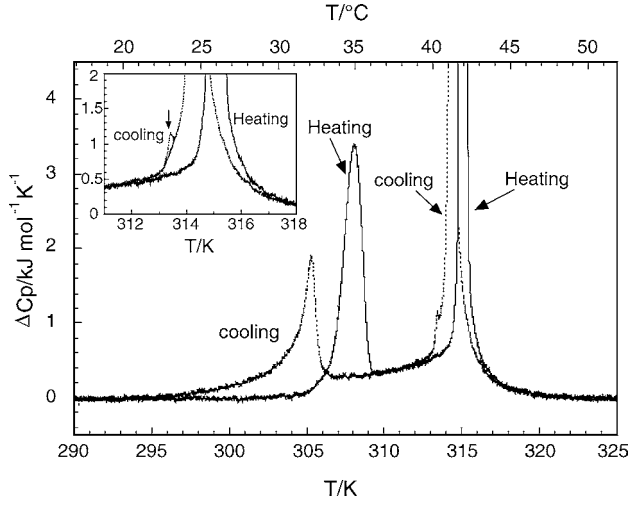

Fig. 5. The magnified figure of the excess heat capacity of DPPC–water–$CaCl_2$ system (Ca/DPPC = 0.042) at the heating/cooling rate of 2 mK s^{-1} (7.2 K h^{-1}). The figure shown in the inset is the magnified one around 315 K. A small peak marked by an arrow shows the sub-main transition.

significantly from pure DPPC. Then, the regular arrangement of the multilamellar structure is deformed. The broadening of the main transition and the interval between the pre-transition and the main transition might be related to such a deformation. The sub-main peak in the cooling run for the sample with Ca/DPPC = 0.164 was larger than that without Ca as seen from Figs. 3 and 6. This behavior is in agreement with the report that the sub-main transition was enhanced by the addition of salt [13,14,18]. The low temperature part of the pre-transition became smaller and the sub-main peak around 315 K became larger with the increase with Ca/DPPC in the cooling run as seen from Figs. 4–6. These behaviors suggest that the pre-transition and the main transition are related with each other, as Heimburg [6,39] reported that the

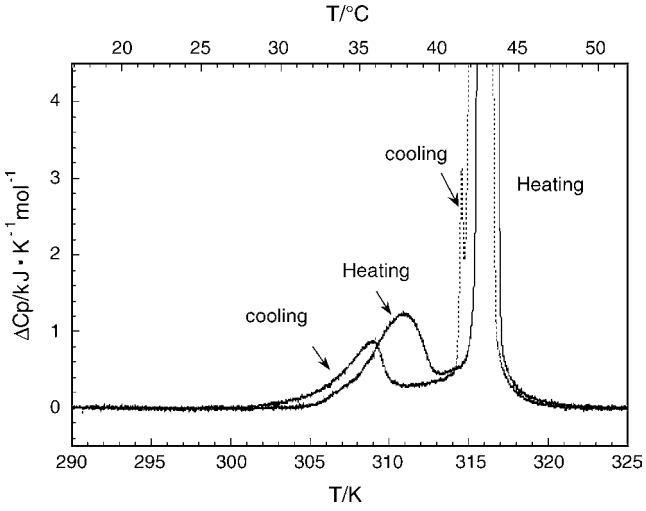

Fig. 6. The magnified figure of the excess heat capacity of DPPC–water–$CaCl_2$ system (Ca/DPPC = 0.164) at the heating/cooling rate of 2 mK s^{-1} (7.2 K h^{-1}).

pre-transition and the main transition were the chain of the events.

At this point, we would like to compare the excess heat capacity of the rippled-gel phase between the heating and cooling run in Figs. 4–6. In DPPC–water system (Fig. 4), the excess heat capacity of the rippled-gel phase in the cooling run is ca. 30 J K^{-1} mol^{-1} larger than that in the heating run, indicating that the metastable rippled-gel phase appeared in the cooling run has a higher energy state. Koynova et al. [35] reported that the excess heat capacity of the metastable rippled-gel phase was ca. 20 J K^{-1} mol^{-1} larger than that of the rippled-gel phase for DPPC and ca. 95 J K^{-1} mol^{-1} larger for distearoylphosphatidylcholine. As the Ca content in DPPC–water–Ca system increases, the excess heat capacity of the metastable rippled-gel phase considerably decreases as compared with the stable rippled-gel phase. The excess heat capacity of the metastable rippled-gel phase obtained in the cooling run was larger than that of the stable rippled-gel phase obtained in the heating run of Ca/DPPC = 0.0 (Fig. 4), became almost the same as that in the heating run of Ca/DPPC = 0.042 (Fig. 5) and then became smaller in the heating run of Ca/DPPC = 0.164 (Fig. 6). The excess heat capacity of the metastable rippled-gel phase obtained in the cooling run is considered to be related with the shoulder in low-temperature part of the pre-transition and the sub-main transition. The excess heat capacity of the metastable rippled-gel phase obtained in the cooling run was large when the shoulder in low-temperature part of the pre-transition was large and the sub-main peak was small, and it became small when the shoulder in low-temperature part of the pre-transition was small and the sub-main peak became large. These behaviors are considered to be originated from the fact that the pre-transition, the sub-main transition and the main transition are the chain of the events and the addition of Ca^{2+} ion affects all these events [19,24].

The binding of Ca^{2+} ion to DPPC lamellar system has been reported to change the surface potential [41], to change the repeat distance of the lamellar phase and deform the molecular arrangement in the bilayers [27], to reduce the motion of phosphate region of polar head group [42], and to decrease the bulk compressional modulus [43]. At the microscopic level, the interaction of Ca^{2+} with the O–P–O and P=O region has been reported to decrease the proportion of the *trans-to-gauche* transition in hydrocarbon chains [42,44], to cause dehydration of lipid bilayer, and to induce structural deformation in the membrane surface through changes in the hydrogen bonding between water and phospholipids [19,43]. Thus, its effects on the repulsive and attractive forces involved in the bilayer–bilayer interaction are considered to affect the stability of the non-rippled gel-phase, the rippled-gel phase and the liquid crystalline phase. The interaction of Ca^{2+} with the lipids is sensitive to the phase state of the bilayer in the order: the gel state > rippled-gel state > liquid crystalline state, according to [19,25]. The change of the stability in these phases due to the interaction of Ca^{2+} with the lipids affects the chain of the transitional events.

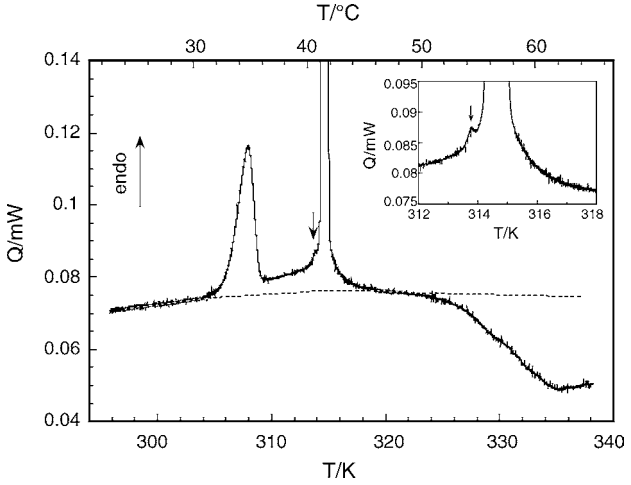

Fig. 7. DSC thermogram of the sonicated sample of DPPC–water system at the heating rate of 2 mK s^{-1} (7.2 K h^{-1}). The figure shown in the inset is the magnified one around 315 K. A small peak marked by an arrow shows the sub-main transition.

The DSC curve for the sonicated sample of DPPC–water system is shown in Fig. 7, where the temperature region measured was up to 338 K. The heat flux shifted to the exothermic side from the temperature region around 325 K both in the heating and cooling run. The heat flux shift to the exothermic side was not observed for the sample without sonication. The sonicated sample is considered to be composed of small unilamellar vesicles (SUV) and the heat flux shift to the exothermic side is due to the heat of coalescence of the small vesicles above 325 K. After the sonicated sample was left at room temperature for 1 month, the heat flux shift to the exothermic side was not observed. This ensures that the coalescence occurs even at room temperature very slowly. In order to investigate the mechanism of the coalescence of the small vesicles, the microscopic observation and the X-ray diffraction study would be necessary. The sub-main transition was also observed in the sample composed of small unilamellar vesicles as shown in the inset in Fig. 7, where it is more clearly seen in the heating run than that of multilamellar vesicles. Since the size and curvature and the interaction with the neighboring bilayer are different between SUV and MLV, these are considered to affect the sub-main transition.

4. Conclusion

The excess heat capacity of the DPPC–water and DPPC–$CaCl_2$ solution system was measured in the both directions of heating and cooling by using a high resolution and high sensitive DSC:

1. A sub-main transition was first observed in the DPPC–water system and this transition was reversible between heating and cooling.
2. The peak due to the pre-transition was different between heating and cooling runs. A shoulder was observed in the low temperature part of the pre-transition peak in the cooling run, which is considered to be due to very slow process of the transition from the metastable rippled-gel to the gel phase.
3. The pre-transition, the sub-main transition and the main transition are considered to be the chain of the events and the addition of Ca^{2+} ion affected all these events. By the addition of Ca^{2+} ion, the shoulder of the pre-transition in the cooling run became smaller and the peak due to the sub-main transition became larger.
4. In the sonicated sample of DPPC–water system, the exothermic effect was observed due to the coalescence of the small vesicles above 325 K.

References

[1] D. Chapman, R. Williams, B.D. Ladbrooke, Chem. Phys. Lipids 1 (1967) 445.
[2] R.B. Geninis, Biomembranes; Molecular Structure and Function, Springer-Verlag, New York, 1989.
[3] R. Koynova, M. Caffrey, Biochim. Biophys. Acta 1376 (1998) 91.
[4] C. Grabielle-Madelmont, R. Perron, J. Colloid Int. Sci. 95 (1983) 471.
[5] M. Kodama, M. Kuwabara, S. Seki, Biochim. Biophys. Acta 689 (1982) 567.
[6] T. Heimburg, J. Biophys. 78 (2000) 1154.
[7] G. Cevc, Biochim. Biophys. Acta 1062 (1991) 59.
[8] S.C. Chen, J.M. Sturtevant, B.J. Gaffney, Proc. Natl. Acad. Sci. U.S.A. 77 (1980) 5060.
[9] H. Yao, H. Nagano, Y. Kawase, K. Ema, Biochim. Biophys. Acta 1212 (1994) 73.
[10] B.G. Tenchov, H. Yao, I. Hatta, Biophys. J. 56 (1989) 757.
[11] H. Yao, S. Matuoka, B. Tenchov, I. Hatta, Biophys. J. 59 (1991) 252.
[12] S. Matuoka, H. Yao, S. Kato, I. Hatta, Biophys. J. 64 (1993) 1456.
[13] K. Pressl, K. Jørgensen, P. Laggner, Biochim. Biophys. Acta 1325 (1997) 1.
[14] C. Trendum, P. Westh, K. Jørgensen, Biochim. Biophys. Acta 1421 (1999) 207.
[15] M. Nielsen, L. Miao, J.H. Ipsen, K. Jørgensen, M.J. Zuckermann, O.G. Mouritsen, Biochim. Biophys. Acta 1283 (1996) 170.
[16] K. Jørgensen, Biochim. Biophys. Acta 1240 (1995) 111.
[17] M.G. Ganesan, D.L. Schwinke, N. Weiner, Biochim. Biophys. Acta 686 (1982) 245.
[18] W.R. Perkins, X. Li, J.L. Slater, P.A. Harmon, P.L. Ahl, S.R. Minchey, S.M. Gruner, A.S. Janoff, Biochim. Biophys. Acta 1327 (1997) 41.
[19] S.A. Tatulian, V.I. Gordeliy, A.E. Sokolova, A.G. Syrykh, Biochim. Biophys. Acta 1070 (1991) 143.
[20] T. Takeda, S. Ueno, H. Kobayashi, S. Komura, H. Seto, Y. Toyoshima, Physica B 213–214 (1995) 763.
[21] H. Minami, T. Inoue, J. Colloid Int. Sci. 206 (1998) 338.
[22] S.A. Simon, L.J. Lis, J.W. Kauffman, Biochim. Biophys. Acta 375 (1975) 317.
[23] D. Chapman, W.E. Peel, B. Kingston, T.H. Lilley, Biochim. Biophys. Acta 464 (1977) 260.
[24] A.C. Biondi, J. Arroyo, S. Diaz, E.A. Disalvo, J. Colloid Int. Sci. 171 (1995) 28.
[25] J. Marra, J. Israelachvili, Biochemistry 24 (1985) 4608.
[26] L.J. Lis, W.T. Lis, V.A. Parsegian, R.P. Rand, Biochemistry 20 (1981) 1771.

[27] Y. Inoko, T. Yamaguchi, K. Furuya, T. Mitsui, Biochim. Biophys. Acta 413 (1975) 24.
[28] S. Hosaka, K. Tozaki, H. Hayashi, I. Inaba, Physica B 337 (2003) 138.
[29] S. Wang, K. Tozaki, H. Hayashi, H. Inaba, J. Thermal Anal. Cal. 79 (2005) 605.
[30] K. Jørgensen, O.G. Mouritsen, Thermochim. Acta 328 (1999) 81.
[31] R.N.A.H. Lewis, N. Mak, R.N. McElhaney, Biochemistry 26 (1987) 6118.
[32] H. Hauser, Chem. Phys. Lipids 57 (1991) 309.
[33] H.-D. Dörfler, P. Miethe, H.W. Meyer, Chem. Phys. Lipids 54 (1990) 181.
[34] S. Kato, T. Kubo, Chem. Phys. Lipids 90 (1997) 31.
[35] R. Koynova, A. Koumanov, B. Tenchov, Biochim. Biophys. Acta 1285 (1996) 101.
[36] A. Blume, Biochemistry 22 (1983) 5436.
[37] D.A. Wilkinson, J.F. Nagel, Biochim. Biophys. Acta 688 (1982) 107.
[38] H.-J. Hinz, J.M. Sturtevant, J. Biol. Chem. 247 (1972) 6071.
[39] T. Heimburg, Biochim. Biophys. Acta 1415 (1998) 147.
[40] W.F. Graddic, J.B. Stamatoff, P. Eisenberger, N. Spielberg, Biochem. Biophys. Res. Comm. 88 (1979) 907.
[41] A.L.Y. Lau, A.C. McLaughlin, R.C. MaDonald, S.G.A. McLaughlin, in: M. Blank (Ed.), Advances in Chemistry Series, vol. 188, American Chemical Society, Washington, DC, 1980, p. 49.
[42] L.J. Lis, J.W. Kauffman, D. Silver, Biochim. Biophys. Acta 406 (1975) 453.
[43] R. Kataoka, S. Aruga, S. Mitaku, K. Kinoshita, A. Ikegami, Biophys. Chem. 21 (1985) 277.
[44] H. Hauser, M.C. Phillips, B.A. Levine, R.P.J. Williams, Eur. J. Biochem. 58 (1975) 133.